ELSEVIER

International Journal of Refractory Metals & Hard Materials 16 (1998) 423–427

International Journal of
REFRACTORY METALS
& HARD MATERIALS

Sintering of alumina–niobium carbide composite

Rosa M. R. Pasotti*, Ana Helena A. Bressiani, José C. Bressiani

Instituto de Pesquisas Energéticas e Nucleares, CP 11049, Pinheiros, CEP 05422-970, Sao Paulo, SP, Brazil

Received 9 March 1998, accepted 8 September 1998

Abstract

Several studies have been focused on particulate-dispersed Al_2O_3 composites in order to improve both room and high temperature mechanical properties and wear resistance. In the present work Al_2O_3–NbC composites have been pressureless sintered and their microstructures analysed as a function of NbC and Y_2O_3 concentration, the latter added as sintering aid. The compositions used in this study were Al_2O_3–xNbC and (Al_2O_3 3%Y_2O_3)–xNbC, (x = 10, 20 and 40 wt%) and the sintering was performed at 1650°C/30 min and 1750°C/15 min. A density greater than 96% of the theoretical density was reached even for those materials sintered at 1650°C. The observed microstructure was more homogeneous for the samples with Y_2O_3 addition and the $Y_3Al_5O_{12}$ phase was detected. The Al_2O_3 grain growth restraining due to the NbC concentration was more pronouncedly in samples sintered at 1750°C

Keywords Ceramic composite, NbC; Alumina, Sintering; Microstructure

1. Introduction

The advent of modern, high-strength, ceramic cutting tools has increased the productivity by allowing materials such as superalloys used in the aerospace industry to be machined at high speeds and has made it possible to machine other hard and strong materials economically [1]. The improved performance of ceramic cutting tools over other tool materials such as cobalt cemented tungsten carbide is due to the ceramic high temperature deformation resistance [2,3]. Alumina-based cutting tools have shown steady improvement in their properties and hence they have experienced growth in their range of application [4,5].

High hardness carbides have been added to alumina in order to improve mechanical and wear properties. The addition of refractory transition metal carbides leads to higher thermal conductivity, presumably because of the formation of a higher conductive intergranular phase [6]. From the mechanical property aspect, these composites exhibit higher hardness and fracture toughness as compared to single phase alumina [7]. The most common carbide added is titanium carbide at a level of 20–40 wt% and the material is normally hot pressed, as reactions between Al_2O_3 and TiC at higher temperatures hamper pressureless sintering [8]. However, plain sintering and sintering followed by hot isostatic pressing, are more desirable fabrication processes, since complex shapes can be economically made and these processes can be used for mass production of near-net-shape materials [9].

Niobium carbide (NbC) has many excellent physico-mechanical properties, such as high melting point, good electric conductivity and high hardness, as TiC does. Besides these properties, the main known world niobium reserves are concentrated in the exceptionally high-grade ore deposits in Brazil (72%) [10]. Owing to these facts a study of NbC–Al_2O_3 composites and a complete microstructure characterization of these materials after pressureless sintering could provide useful technological information. In the present work, alumina–niobium carbide samples were pressureless sintered in order to determine the densities and to investigate the microstructure characteristics as a function of Y_2O_3 addition [11,12].

2. Experimental procedure

Samples were prepared by using the usual ceramic processing techniques. Al_2O_3 and NbC powders with average sizes of 0.37 and 2.3 μm respectively were

*Corresponding author. Tel.: +55-11-8169369; fax: +55-11-8169370, e-mail: rpasotti@net.ipen.br

0263-4368/98/$ — see front matter
PII S0263-4368(98)00053-5

used. Three wt% of Y_2O_3 was added to Al_2O_3 and ball-milled for 10 h by using Al_2O_3 grinding medium. The powder compositions used in this study were Al_2O_3–xNbC and ($Al_2O_3$3%Y_2O_3)–xNbC, where x = 10, 20 and 40 wt%.

The powders were pressed in a die of approximately 12 mm in diameter to obtain pellets which were further pressed isostatically at 200 MPa. The composites were embedded in powders of the same composition and then sintered in a graphite-resistance-heated furnace with flowing argon at 1650°C/30 min and 1750°C/15 min. The heating and cooling rates were 20°C/min.

After sintering, the top surface layers were removed from the samples by grinding, and the relative densities were measured by the Archimedes method. X-ray diffraction (XRD) was used to identify crystalline phases. To evaluate the grain structure, the polished surfaces of the specimens were observed by using a scanning electron microscope (SEM) after thermal etching at 1450°C for 0.5 h under vacuum. Transmission electron microscopy (TEM) was used to investigate the formed phases and for a full microstructural characterization. Samples for TEM analyses were prepared by using a conventional thinning procedure that included dimple grinding and finally argon ion milling.

3. Results and discussion

X-ray diffraction patterns of the composites after sintering indicated the presence of α-Al_2O_3 and NbC. However, the $Y_3Al_5O_{12}$ (YAG) phase was also detected in the specimens containing Y_2O_3 and no evidence of any other phase was found. The phase diagrams for the Y_2O_3–Al_2O_3 system indicate a fair solubility of yttria into alumina [13], and the formation of the YAG phase is likely due to a eutectic reaction between Al_2O_3 and Y_2O_3 close to 1760°C. Figure 1 shows the XRD pattern of (Al_2O_3 3 wt%Y_2O_3)–10NbC composite sintered at 1750°C/30 min.

The specimens showed remarkable relative densities, higher than 96% of theoretical density even for the samples sintered at 1650°C (Table 1). These density values indicate that pores have been completely closed, which is a necessary condition for further densification by hot isostatic pressing (HIP) without encapsulation [14]. In the present work higher relative density values are accomplished for Al_2O_3–NbC composites when compared to more common Al_2O_3–TiC pressureless sintered composites [15].

The densification of samples containing Y_2O_3 was slightly higher than for those without Y_2O_3. The sintering of Al_2O_3–NbC composites with Y_2O_3 additions at high temperatures is expected to occur in the presence of liquid phases and to lead to higher densities. For the specimens with additives sintered at 1650°C/30 min the density values decreased as the NbC concentration was raised, while densities of specimens sintered at 1750°C/15 min did not have a large variation.

Except for samples with 40% NbC sintered at 1750°C, the density values remained almost the same regardless of the Y_2O_3 addition. However, the microstructure seemed to be greatly affected by the Y_2O_3 presence (Fig. 2). For samples containing Y_2O_3 the microstructure is more homogeneous and the NbC grains are located at the Al_2O_3 grain boundaries [Fig. 2(b)]. The microstructures of samples without Y_2O_3 show NbC clusters and Al_2O_3 grain size comparatively smaller than for those ones with additive [Fig. 2(a)].

The medium Al_2O_3 grain size as a function of the NbC concentration and the temperature has been measured by using the Quantikov's method [16]. Table 2 shows the medium grain diameter of alumina for ($Al_2O_3$3%Y_2O_3)–xNbC and Al_2O_3–xNbC, where x = 10, 20 and 40% NbC. As the NbC concentration is raised, the growth of Al_2O_3 grains in the matrix is

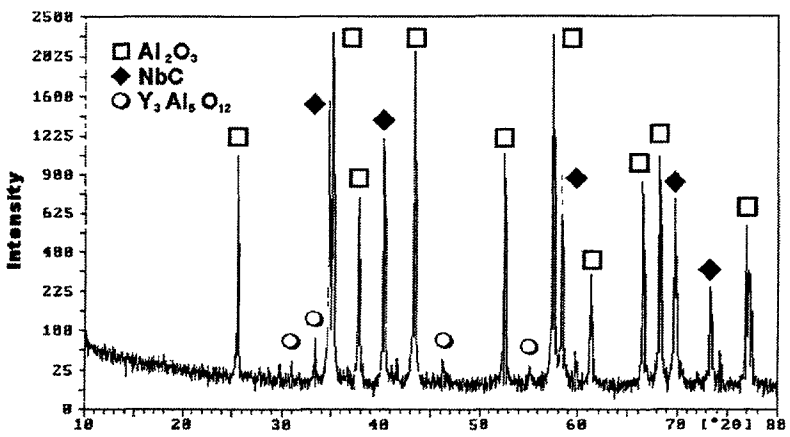

Fig. 1 X-ray diffraction pattern of the ($Al_2O_3$3%Y_2O_3)10NbC composite

Table 1
Relative apparent densities of Al_2O_3–NbC composites after sintering

Sample	% Theoretical density (TD) 1650°C/30 min	%Theoretical density (TD) 1750°C/15 min
Al_2O_3–10NbC	98 0	97.6
(Al_2O_3 $3Y_2O_3$)10NbC	98.8	98 4
Al_2O_3–20NbC	97.5	98.2
(Al_2O_3 $3Y_2O_3$)20NbC	98 0	98.6
Al_2O_3–40NbC	96 0	96 2
(Al_2O_3 $3Y_2O_3$)40NbC	96 1	98 1

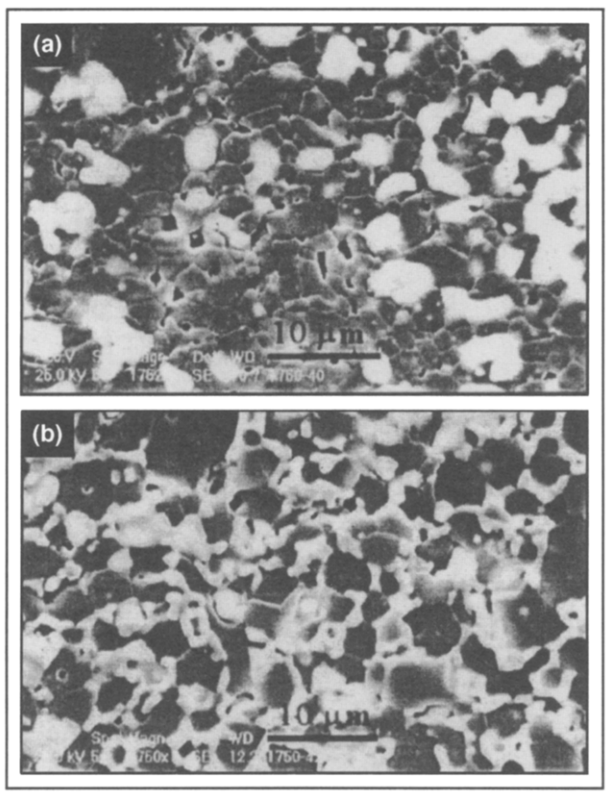

Fig 2 Microstructure of Al_2O_3–40NbC. (a) 0% Y_2O_3, and (b) 3% Y_2O_3, sintered at 1750°C (white grains: NbC; grey grains Al_2O_3)

Table 2
Medium Al_2O_3 grain size as a function of NbC concentration

Sampled	d (μm) 1650°C/30 min	d (μm) 1750°C/15 min
Al_2O_3–10NbC	1.4±0 8	2 6±1 4
(Al_2O_3 $3Y_2O_3$)10NbC	1 6±0 9	4 1±2 5
Al_2O_3–20NbC	1.3±0.9	2 3±1.4
(Al_2O_3 $3Y_2O_3$)20NbC	1.4±0 7	2.4±1.8
Al_2O_3–40NbC	1 3±0 7	1.8±0 9
(Al_2O_3 $3Y_2O_3$)40NbC	1.4±0.7	1.9±0.9

Table 3
Medium NbC grain size as a function of its concentration in the composites

Al_2O_3–xNbC	Without Y_2O_3	With Y_2O_3
x = 10%	1 8±0.9	1 5±0 8
x = 20%	2 4±1 1	1.8±0 9
x = 40%	2.4±1 0	1.7±0.6

restrained by the introduction of a second phase. This effect was more pronounced for samples sintered at 1750°C/15 min. On the other hand, for composites sintered at 1650°C/30 min the variation of the medium grain size was very small regardless of the NbC concentration and Y_2O_3 addition.

The medium NbC grain size has been also measured for composites sintered at 1750°C/15 min with and without Y_2O_3 (Table 3). The results indicate that the presence of yttria leads to a finer distribution of NbC grain size and the medium grain size values are almost the same regardless of the NbC concentration.

The differences in the microstructure as a function of NbC concentration and temperature can be visualized in Figure (3). Samples (Al_2O_3 3% Y_2O_3)10 NbC and (Al_2O_3 3% Y_2O_3)20NbC sintered at 1650°C, corresponding to Figs 3(a) and 3(c) respectively, exhibited homogeneous microstructures. The Al_2O_3 grain size is notably different from the ones originating from samples sintered at 1750°C/15 min with the same composition [Figs 3(b) and 3(d)]. We also observed that the Al_2O_3 grain size decreases as the NbC concentration is raised, better seen in Figs 3(b) and 3(d).

The microstructure observed by TEM was consistent with three phases, that is, Al_2O_3, NbC and YAG. The grain distribution of NbC and Al_2O_3 was observed without the objective aperture of the objective lens and the phases identification by using the selected area electron diffraction patterns. The YAG phase, which was probably crystallized from a liquid phase during cooling, was located within Al_2O_3 grain triple junction. Its structure is body centred cubic (bcc) with 1.201 nm lattice parameter. Figure 4 shows the YAG phase in both bright field and corresponding dark field images. The dark field was obtained from a spot of the electron diffraction pattern [Fig. 5(b)]. The diffraction spots are shown in Fig. 5(b) with the [4 1 −2] direction of the incident electron beam and Fig. 5(a) shows the same diffraction pattern indexed by a software (DIFPAT)†. Structure details such as grain boundary nature determination (amorphous, crystalline) and the search for any other phase have not yet been done.

†Software developed by Graham Carpenter and Laris Benkins at the Metals Technology Laboratories, CANMET, Energy Mines and Resources — Ottowa, Canada

4. Conclusions

Al_2O_3–NbC composites have been obtained by pressureless sintering with high relative densities (> 96% TD) even for those materials sintered at 1650°C. The addition of Y_2O_3 in small amounts (3 wt% into the Al_2O_3) is effective for the densification of Al_2O_3–NbC composites. Densities of 98% TD have been reached except for samples with 40% NbC sintered at 1650°C.

The microstructures of Al_2O_3–NbC composites were homogeneous and the NbC grains were located along the Al_2O_3 grain boundaries for samples containing Y_2O_3. The increasing concentration of NbC leads to an Al_2O_3 grain growth restraining, therefore better mechanical properties can be achieved. This effect has been observed more pronouncedly in samples sintered at 1750°C while for samples sintered at 1650°C the Al_2O_3 grain size hardly changed. Considering that one of the most effective way to control the grain growth is

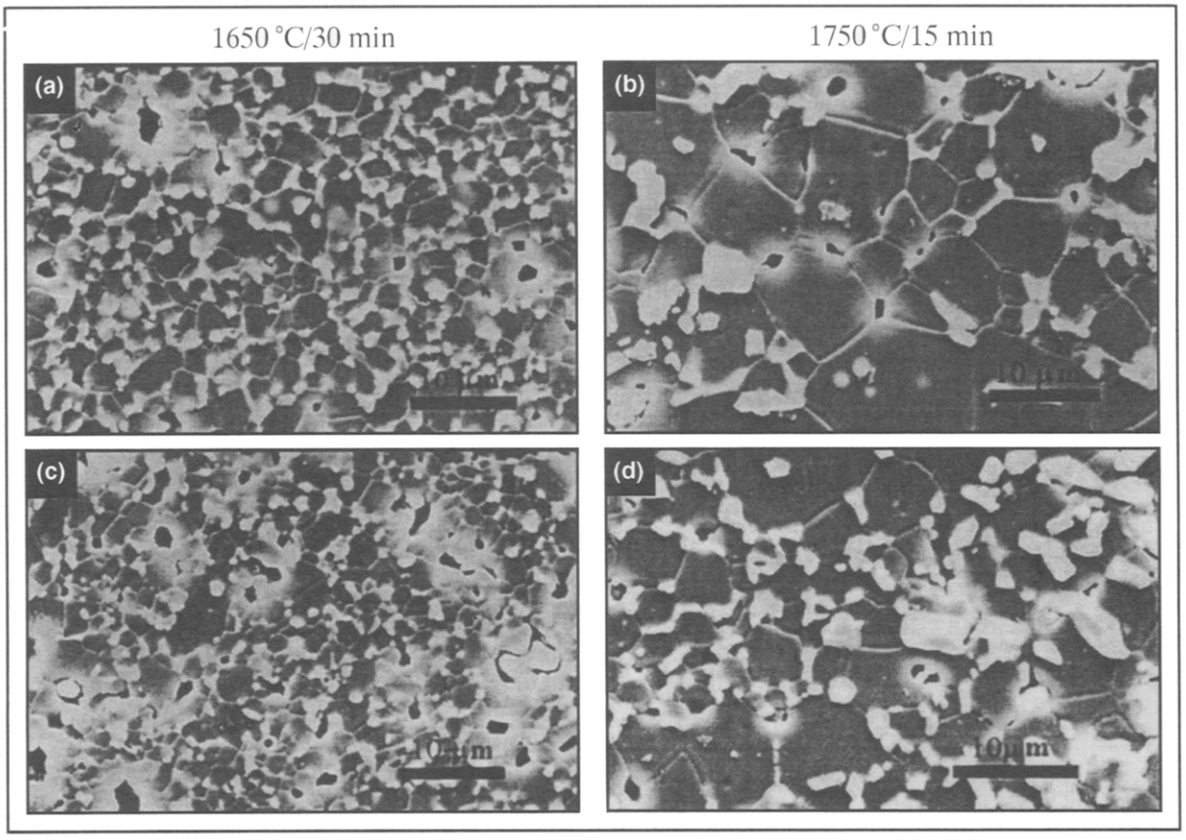

Fig. 3. SEM images of etched polished surfaces of $(Al_2O_3 3\%Y_2O_3)$–x NbC· (a) and (b) x = 10%, (c) and (d) x = 20%.

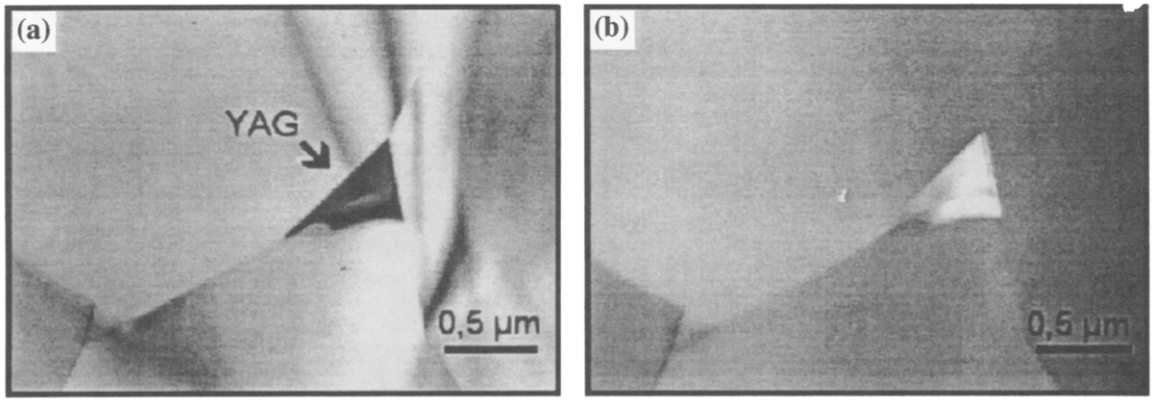

Fig 4. $Y_3Al_5O_{12}$ (YAG) phase located within Al_2O_3 grain triple junction: (a)bright field, (b) dark field.

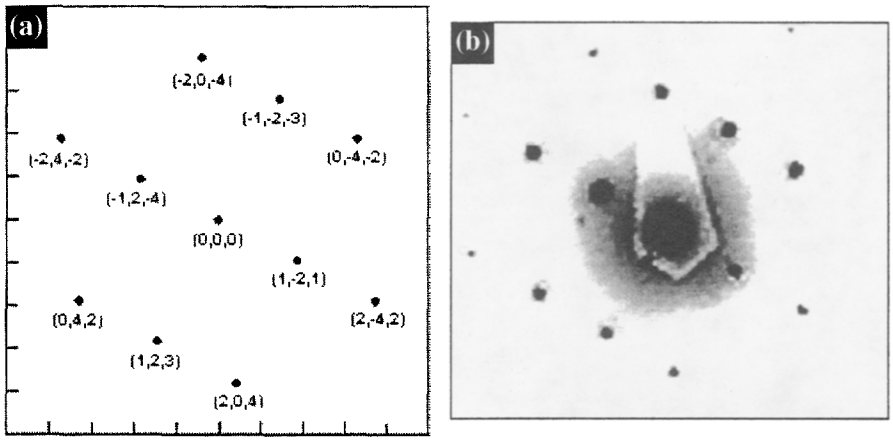

Fig 5 (a) YAG phase diffraction pattern indexed by DIFPAT software (B = [4 1 −2]); (b) diffraction pattern of YAG phase get from (Al_2O_3 3%Y_2O_3)10NbC sample, sintered at 1750°C/15 min (negative of digital image)

by keeping the sintering temperature as low as possible, setting it to 1650°C was found to be suitable, since the composite densities reached were high enough to perform a further densification by HIP.

In the (Al_2O_3 3%Y_2O_3)NbC samples the liquid phase generated by the heating process has been crystallized during cooling. From the X-ray diffraction the presence of YAG ($Y_3Al_5O_{12}$) has been detected and found to be located within Al_2O_3 grain triple junctions and at grain boundaries by the TEM analyses.

Acknowledgements

The authors acknowledge the 'Programa de Apoio ao Desenvolvimento Científico e Tecnológico' (PADCT/Finep), 'Conselho Nacional de Desenvolvimento Científico e Tecnológico' (CNPq), and 'Fundaçcão de Amparo a Pesquisa do Estado de São Paulo' (FAPESP) for the financial support. Thanks also to Dr Martinelli for helping in the English redaction.

References

[1] Chuznzhen H, Xing A, Zhaoqian L. Cutting performance of advanced ceramic tools. Am Ceram Soc Bull 1997,76·83–5
[2] Warren R (editor) Ceramic-matrix composites New York Chapman and Hall, 1992.
[3] Baldoni JG, Buljan ST Ceramic for machining Am Ceram Soc Bull 1988,67:381–7
[4] Furukawa M. Alumina ceramic tools. Am Ceram Soc Bull 1988,62·1384–86
[5] Burden SJ, Hong J, Rue JW. Comparison of hot-isostatically-pressed and uniaxially hot-pressed alumina–titanium carbide cutting tools Am Ceram Soc Bull 1988,67 1003–5
[6] Cutler RA, Hanford AC. Pressureless-sintered Al_2O_3–TiC composites Mater Sci and Engng 1988;105–106·183–92.
[7] Wari RP, Ilschner B. Fracture behaviour of composites based on Al_2O_3–TiC J Mater Sci 1980,15.875–85
[8] Wook YK, Gunn JL. Pressureless sintering of alumina titanium carbide composites. J Am Ceram Soc 1989;72.1333–7.
[9] Borom MP, Lee M. Effect of heating rate on densification of alumina–titanium carbide composites Ceram Mater 1986, 1:335–40.
[10] Lyakishev NP, Tulin N, Pliner YL. Niobium in steels and alloys São Paulo.CBMM, 1984:1–14.
[11] Chae KW, Yeon D. Effect of Y_2O_3 additions on the densification of an Al_2O_3–TiC composite. J Am Ceram Soc 1993,76·1857–60.
[12] Chae KW, Yeon D Sintering of Al_2O_3–TiC composite in the presence of liquid phase J Am Ceram Soc 1995;78·257–9
[13] Levin EM, Robbins CR, McMurdic HF. In Reser MK, editor. Phase diagrams for ceramists Columbus, OH Americam Ceramic Society, 1964 122 (Fig. 311)
[14] Kwon ST, Kim DY, Kang TK, Yoon DN. Effect of sintering temperature on the densification of Al_2O_3 J Am Ceram Soc 1987,70:69–70
[15] Ishigaki T, Sato K, Moriyoshi Y. Pressureless sintering of TiC–Al_2O_3 composites J Mater Sci Lett 1989,8·678–80.
[16] Pinto LCM, Vasconcelos V, Vasconcelos WL, Bressiani JC An algorithm of digital image processing applied to quantification of grains with discontinuos boundaries Acta Microscopica Suppl B;1996.168–9